Low-Complexity Channel Estimation in OFDM MU-MIMO Next Generation Cellular Networks

Marco Martalò,[1] Alessandro Opinto,[1] Marco Maso,[2] Mérouane Debbah,[2] and Riccardo Raheli[1]
1: Department of Engineering and Architecture, University of Parma, Italy
2: Mathematical and Algorithmic Sciences Lab, Huawei Paris Research Center, France
{marco.martalo,riccardo.raheli}@unipr.it, alessandro.opinto@studenti.unipr.it, {marco.maso,merouane.debbah}@huawei.com

***Abstract*—We consider downlink communications between a Base Station (BS) and various mobile stations, equipped with multiple antennas, based on Orthogonal Frequency Division Multiplexing (OFDM). Transmission is compliant with the Long Term Evolution (LTE) standard operating in Frequency Division Duplex (FDD) mode. Since ideal feedback of channel state information to the BS may be cumbersome, we consider two suboptimal channel estimation algorithms, denoted as Resource Block (RB) and Resource Block Group (RBG). Both approaches approximate the channel as constant over multiples of the fundamental LTE block, known as Physical Resource Block (PRB). Our results show that RB and RBG incur a limited performance loss, yet guaranteeing significant saving in the amount of feedback information.**

I. Introduction

Mobile communication systems have evolved to cope with the growth of data traffic and number of mobile devices. According to CISCO estimates [1], mobile data traffic has grown 18-fold between 2012 and 2016 and is expected to further increase 7-fold until 2021. To enable this growth, a fifth generation cellular network (5G) is therefore needed [2]. Since one of the key goals of 5G is to improve the user spectral efficiency by an order of magnitude, Multiple Input Multiple Output (MIMO) techniques, with a possibly large amount of antenna elements at the Base Station (BS), e.g., the so-called massive MIMO, may represent an effective approach [3].

In downlink MIMO communications, the BS transmits to Mobile Stations (MSs) through channels affected by fading and Additive White Gaussian Noise (AWGN). An effective transmission, which is here analyzed, exploits Orthogonal Frequency Division Multiplexing (OFDM) operating in Frequency Division Duplex (FDD) in a way compliant with the Long Term Evolution (LTE) standard [4]. In order to estimate the communication channel, the BS sends to each MS pilot symbols, known to both sides. Once the MS processes them, quantized Channel State Information at the Transmitter (CSIT) is provided to the BS, which uses it for precoding setting.

In FDD mode, the conventional overhead for the CSIT acquisition grows linearly with the sum of the number of BS antennas and MSs scheduled for downlink transmission. Therefore, it can rapidly become unmanageable for massive MIMO systems [5]. Several approaches to mitigate this problem have been proposed in the literature, see, e.g., [6] and references therein. Most of these solutions propose effective suboptimal channel estimation strategies that exploit the high correlation which typically characterizes the channels observed by each transmit/receive antenna pair in massive MIMO systems. Channel estimation is a hot topic also for OFDM-based MIMO communication systems and various solutions have been proposed in the literature. An exhaustive review on the topic may be found, e.g., in [7].

In this paper, we focus on two suboptimal, in terms of Bit Error Rate (BER), yet computationally feasible, channel estimation algorithms for OFDM-based Multi-User (MU) MIMO communications. These algorithms are based on the LTE downlink frame structure, which is composed of a fundamental block of 12 subcarriers in a downlink slot, denoted as Physical Resource Block (PRB). In the first algorithm, referred to as Resource Block (RB), the channel is supposed to be constant over one PRB, i.e., the coherence bandwidth of the channel is supposed to be larger than one PRB. As a consequence, the channel response over the entire PRB is approximated with that observed in a subcarrier of that PRB. The second strategy, referred to as Resource Block Group (RBG), extends the RB algorithm by averaging the channel estimates over consecutive PRBs and using only one value for all the subcarriers in the grouped PRBs. Note that the terminology RBG is reminiscent of the Resource Allocation Type 0 (RAT0) in the LTE standard, which defines how groups of PRB resources can be allocated to different users [8].

Our results show that RB and RBG channel estimation algorithms guarantee an effective tradeoff, with respect to ideal channel estimation, between the loss in performance and saving in feedback information size. Besides being valid for LTE networks, this result indicates that the considered suboptimal algorithms may also serve as possible solutions for future 5G networks, whose physical layer is expected to be based on OFDM [9].

II. System Model

A. The LTE Standard

We first recall the structure of the downlink LTE frame employed in this work, which is at the basis

The work of Alessandro Opinto was performed during an internship at the Mathematical and Algorithmic Sciences Lab, Huawei Paris Research Center, France.

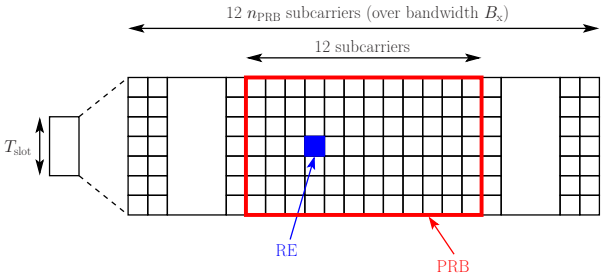

Fig. 1. Time-frequency resource grid in an LTE downlink slot.

TABLE I
LTE CHANNEL BANDWIDTHS AND NUMBER OF PRBS.

Channel Bandwidth B_{x} [MHz]	Number of PRBs n_{PRB}
1.4	6
3	15
5	25
10	50
15	75
20	100

of the considered channel estimation suboptimal algorithms [10]. The LTE standard in FDD mode foresees a downlink frame, of size $T_{\mathrm{frame}} = 10$ ms, divided into 10 subframes, each of duration $T_{\mathrm{sub}} = T_{\mathrm{frame}}/10 = 1$ ms. The single subframe is then divided into 2 slots of duration $T_{\mathrm{slot}} = T_{\mathrm{sub}}/2 = 0.5$ ms each.

According to OFDM modulation, one slot has a time-frequency resource grid as depicted in Fig. 1, where subcarriers are equally spaced by 15 kHz. In this context, the PRB is the fundamental block of resources which can be allocated to a user. One PRB consists of 12 consecutive subcarriers (or, equivalently, 180 kHz) in a slot and is composed of Resource Elements (REs), which are the smallest time-frequency elements belonging to the PRB. The number of the REs that can be contained in a PRB depends on the used Cyclic Prefix (CP). Although the standard envisions two types of CP insertion, in this work we consider the presence of 7 OFDM symbols per subcarrier in a slot, as depicted in Fig. 1. In this case, one LTE downlink frame contains 140 OFDM symbols per subcarrier transmitted in 10 ms.

Channel bandwidths from 1.4 MHz up to 20 MHz are available. Note that the latter bandwidth is used to achieve the highest LTE data rate. Such bandwidths and the corresponding number of PRBs are summarized in Table I.

B. OFDM MU-MIMO Downlink

We consider a scenario where a BS, equipped with N_{t} transmitting antennas, is placed at the center of a circular cell. BS antennas are sectorized, so that 3 equal sectors of 120 degrees each are covered. In the cell, N_{u} MSs, each equipped with N_{r} receiving antennas, are equally divided among sectors. The distance of each MS from the BS is modeled as a random variable with uniform distribution in the interval $[R_{\min}, R_{\max}]$, whereas the angle within each sector is modeled as a random variable with uniform distribution in the interval $[0, 120]$ degrees.

The system model for the considered OFDM MU-MIMO downlink transmission from the BS to a MS is depicted in Fig. 2. At the BS (left-hand side of Fig. 2), the information sequence to be transmitted, denoted as $\{b_k\}$, is composed of K linearly modulated symbols, e.g, by Quadrature Amplitude Modulation (QAM). Such a sequence is parallelized into N_{c} subcarriers. At this stage, data is framed according to the LTE standard, as described in Section II-A. Scheduling then allocates subcarriers to users according to the algorithms described in Section III.

Once CSIT is available, data may be adapted to the channel by means of precoding. In this work, well-known linear precoders have been investigated, i.e., Maximum Ratio Transmission (MRT), Zero-Forcing (ZF), and Regularized Inverse (RI) [11].

OFDM symbols are generated in parallel for all the N_{t} antennas. In each antenna branch, an Inverse Discrete Fourier Transform (IDFT) is first performed on the N_{c} input symbols, each loaded on one subcarrier. Then, the CP is added at the beginning of the sequence of N_{c} time-domain samples, in the form of the copy of the last N_{g} samples. This operation is necessary to mitigate the impact of channel dispersion on the system performance. Finally, the obtained N_{t} OFDM symbols, each composed of $N_{\mathrm{c}} + N_{\mathrm{g}}$ samples, are transmitted by the BS over the N_{t} antennas.

The transmitted signal can be represented as the sum of the signals transmitted by the N_{t} antennas and it can be obtained by means of linear operations, as in the following. Consider the downlink transmission of a single LTE slot and denote as $\boldsymbol{D}$ the complex matrix, of size $N_{\mathrm{c}}N_{\mathrm{r}} \times 7$, containing the OFDM symbols. With some manipulations, the matrix of transmitted symbols, of size $(N_{\mathrm{c}} + N_{\mathrm{g}})N_{\mathrm{t}} \times 7$, can be written as

$$\boldsymbol{X} = \boldsymbol{A}\boldsymbol{F}^{-1}\boldsymbol{W}\boldsymbol{D} \tag{1}$$

where $\boldsymbol{W} \in \mathbb{C}^{N_{\mathrm{c}}N_{\mathrm{t}} \times N_{\mathrm{c}}N_{\mathrm{r}}}$ implements the considered precoding strategies, $\boldsymbol{F}^{-1} = \boldsymbol{F}_{\mathrm{d}}^{-1} \otimes \boldsymbol{I}_{N_{\mathrm{t}}} \in \mathbb{C}^{N_{\mathrm{c}}N_{\mathrm{t}} \times N_{\mathrm{c}}N_{\mathrm{t}}}$ performs the IDFT, $\otimes$ and $\boldsymbol{I}_n$ denote the Kronecker product between matrices and the identity matrix of dimension n, respectively, $\boldsymbol{F}_{\mathrm{d}}^{-1}$ is the inverse of the DFT matrix on a single antenna with elements $\boldsymbol{F}_{\mathrm{d}}^{(i,k)} = e^{-j2\pi ik}/\sqrt{N_{\mathrm{c}}}$, for $i, k = 0, 1, \ldots, N_{\mathrm{c}} - 1$, and $\boldsymbol{A} \in \mathbb{R}^{(N_{\mathrm{c}}+N_{\mathrm{g}})N_{\mathrm{t}} \times N_{\mathrm{c}}N_{\mathrm{t}}}$ implements the CP insertion and is defined as

$$\boldsymbol{A} = \begin{bmatrix} \boldsymbol{0}_{(N_{\mathrm{g}}N_{\mathrm{t}}) \times (N_{\mathrm{c}}-N_{\mathrm{g}})N_{\mathrm{t}}} & \boldsymbol{I}_{N_{\mathrm{g}}N_{\mathrm{t}}} \\ & \boldsymbol{I}_{N_{\mathrm{c}}N_{\mathrm{t}}} \end{bmatrix}$$

being $\boldsymbol{0}_{m \times n}$ the all-zero m-by-n matrix.

At the MS (right-hand side of Fig. 2), the following received complex matrix, of size $(N_{\mathrm{c}} + N_{\mathrm{g}})N_{\mathrm{r}} \times 7$, is observed

$$\boldsymbol{Y} = \boldsymbol{H}\boldsymbol{X} + \boldsymbol{N}$$

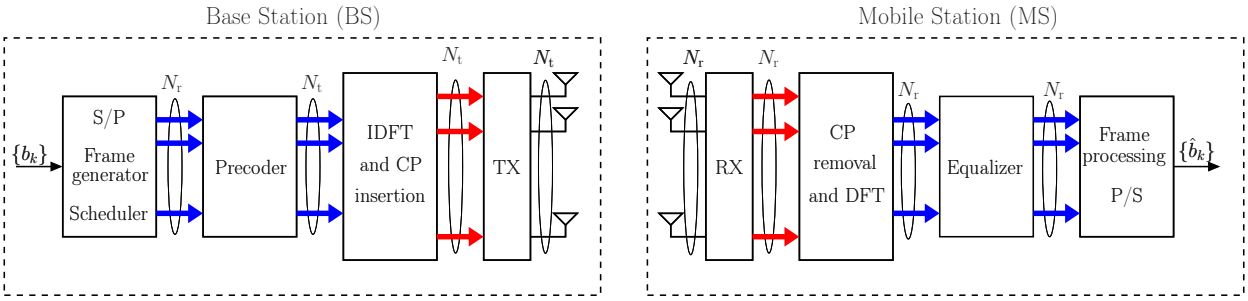

Fig. 2. System model for the considered OFDM MU-MIMO downlink system. Thicker lines correspond to vectors of OFDM symbols for each antenna, with size N_c (blue lines) or $N_c + N_g$ (red lines).

in which $\boldsymbol{N} \in \mathcal{CN}(\boldsymbol{0}, N_0\boldsymbol{I})$ and the channel matrix $\boldsymbol{H} \in \mathbb{C}^{(N_c+N_g)N_r \times (N_c+N_g)N_t}$ can be shown to be block circulant [12] and uniquely identified by the first column, of size $(N_c + N_g)N_r \times N_t$, which is equal to

$$\left[\boldsymbol{H}_1^T, \boldsymbol{H}_2^T, \ldots, \boldsymbol{H}_L^T, \boldsymbol{0}^T\right]^T$$

where T is the transpose operator, L is the number of taps describing the fading channel, and $\boldsymbol{H}_i$, $i = 1, 2, \ldots, L$, are circularly symmetric complex Gaussian matrices, of size $N_r \times N_t$, with unitary variance.

Similarly to the operations performed at the transmitter, the first operations on the received frame are the OFDM CP removal and the DFT. In order to cope with the errors possibly introduced by the precoder due to non-perfect channel estimation, equalization of the received frame is needed. In this work, classical ZF and Minimum Mean Square Error (MMSE) equalization strategies are considered [13]. Finally, an estimate of the transmitted sequence, denoted as $\{\hat{b}_k\}$, is provided. Note that a linear formulation of the operations at the MS, similar to that in (1), can be also given, by means of properly chosen matrices $\boldsymbol{B}$, $\boldsymbol{F}$, and $\boldsymbol{Q}$ representing CP removal, DFT, and equalization operations, respectively.

III. Low-Complexity Channel Estimation and Resource Allocation

Channel estimation is performed by resorting to proper pilot symbols known to both BS and MSs. Unlike the LTE standard, which defines positions in the transmitted frame for these symbols, in this work we assume, for simplicity, that channel estimation is performed before data transmission. However, we note that the adopted ratio between number of pilots and number of data symbols is the same as in the LTE standard. Thus our choice is only made for the sake of simplicity of the implementation but is quantitatively compatible with LTE standard. Upon reception, the MS processes the received pilot symbols using standard MMSE estimation and feeds back quantized CSIT to the BS.

In an ideal estimation algorithm, all the channel coefficients between each pair of transmit/receive antennas in all subcarriers can be estimated. However, such an approach leads to the backward transmission of a huge amount of CSIT. In this strategy, the MS has to feed back one symbol for each channel coefficient between each pair of transmit/receive antennas in all REs. This means that the feedback size, i.e., the total number of symbols fed back by each scheduled MS to the BS, is equal to

$$n_{\mathrm{f,ideal}} = N_c N_t N_r = 12 n_{\mathrm{PRB}} N_t N_r.$$

In practice, this option is unfeasible in the majority of the cases, thus it is considered only as a benchmark for the BER performance of the considered schemes.

In order to reduce the complexity of the channel estimation algorithm, and the consequent feedback size, we now exploit the LTE downlink frame structure described in Section II-A. In particular, one can assume the presence of a constant channel gain across the subcarriers spanning a PRB and, therefore, approximate the channel gains over the entire PRB with the channel gain of one of its subcarriers. We denote this estimation technique as RB. This approach is expected to yield higher BER with respect to the ideal case due to reduced quality in channel estimation. However, it allows a reduction of the size of the feedback to be transmitted from the MS to the BS. In particular, it can be shown that the feedback size is equal, in this case, to

$$n_{\mathrm{f,RB}} = n_{\mathrm{PRB}} N_t N_r = n_{\mathrm{f,ideal}}/12$$

i.e., a 12-fold reduction can be achieved.

A further reduction, at the cost of an additional loss in estimation precision, can be achieved by extending the RB algorithm as follows. Instead of estimating the channel coefficients separately in each PRB, K_{RBG} PRBs are bundled together and their RB channel gains are averaged to yield a unique estimation for the group of PRBs, valid for each RE of the group itself. This approach is denoted as RBG.

The parameter K_{RBG} is fixed according to the specifications given in the LTE standard for the RAT0, which defines possible assignment of block of PRBs to a unique user based on the channel bandwidth. In

TABLE II
CONSIDERED SIMULATION SETUPS.

Parameter	Scenario 1	Scenario 2
$N_{\mathrm{t}} \times N_{\mathrm{r}}$	32×2	2×2
B_{x}	3 MHz	10 MHz
K_{RBG}	2	3
Propagation models	EVA [14]	ETU [14]
Pathloss model	ITU-R commercial [15]	
Modulation	64-QAM	
N_{u}	6	
$R_{\min}, R_{\max}$	30, 120 m	
User speed	4 km/h	

particular, PRBs are grouped for channel estimation as in RAT0. With reference to Table I, $K_{\mathrm{RBG}} = 1$ in the first channel bandwidth, $K_{\mathrm{RBG}} = 2$ in the second and third bandwidth, $K_{\mathrm{RBG}} = 3$ in the fourth bandwidth, and $K_{\mathrm{RBG}} = 4$ in the fifth and sixth bandwidth. Note that for $B_{\mathrm{x}} = 1.4$ MHz, RB and RBG estimation techniques coincide. If $n_{\mathrm{PRB}}/K_{\mathrm{RBG}}$ is not an integer, ad hoc grouping can be considered. As an example, for $B_{\mathrm{x}} = 3$ MHz, $n_{\mathrm{PRB}} = 15$, $K_{\mathrm{RBG}} = 2$ and 7 pairs of PRBs are grouped according to the RBG algorithm described above, while the last PRB is processed individually as in RB.

Finally, in the RBG approach the MS feeds back to the BS a number of symbols equal to

$$n_{\mathrm{f,RBG}} = N_r N_t \left\{ \left\lfloor \frac{n_{\mathrm{PRB}}}{K_{\mathrm{RBG}}} \right\rfloor + \mathrm{mod}\left(n_{\mathrm{PRB}}, K_{\mathrm{RBG}}\right) \right\}$$

where $\mathrm{mod}(x, N) = x - \lfloor n/N \rfloor N$ stands for the modulo operation, being $\lfloor x \rfloor$ the largest integer less than or equal to x. In other words, the term $\mathrm{mod}(n_{\mathrm{PRB}}, K_{\mathrm{RBG}})$ takes into account the fact that $n_{\mathrm{PRB}}/K_{\mathrm{RBG}}$ may not be integer. In this case, the feedback size can be reduced, with respect to the RB algorithm, by a factor on the order of K_{RBG}.

As described in Fig. 2, at the BS a scheduler allocates the resources (subcarriers) to specific users in the area. Since the design of a novel scheduler is beyond the scope of this paper, we consider a simplified scheduler, which allocates to each user an amount of resources equal to the number of separately estimated subcarriers.

For ideal channel estimation, the channel coefficient is estimated in each single subcarrier. Therefore, each subcarrier is randomly and uniformly allocated to a user. The BS does not store any information about the users served in a given slot. In fact, in the considered scenario the number of available subcarriers is sufficiently large with respect to the number of users so that all users are served in a given slot with high probability.

For RB channel estimation, a single channel coefficient is estimated for an entire PRB. Therefore, the scheduler randomly allocates each PRB to a user and the average number of served users in each slot is fixed. Unlike the ideal case, it may happen that, if the number of users is larger than the available PRBs, some of them may not be served in a given slot. In order to improve the fairness among the users, the BS stores information about the users served in the past slots, so that in the present slot priority is given to less served users.

For RBG channel estimation, scheduling is similar to that used for RB channel estimation, the only difference being the fact that the minimum resource which can be allocated to a user is a group of PRBs. Therefore, a fairness similar to that of RB can be achieved in this case as well.

IV. NUMERICAL RESULTS

As illustrative examples, we now present simulation results about the considered MU-MIMO OFDM downlink communication system for two scenarios summarized in Table II. These scenarios are representative of communications in an indoor femtocell through moderately and severely frequency-selective channels, respectively. In order to obtain statistically meaningful results, 10^6 bits are transmitted and various independent realizations of AWGN and fading are generated. These values are chosen to obtain a tradeoff between simulation accuracy and duration. Finally, the BER is calculated as the average over all the users in the cell (whose positions are generated as described in Section II-B) and results are presented as functions of the received Signal-to-Noise Ratio (SNR) after equalization.

In Fig. 3, the BER is shown, as a function of the SNR, for the first simulation scenario in Table II. The presented channel estimation algorithms are considered with MMSE equalizer and different precoders: (a) ZF and (b) RI. One can observe that in both cases RB and RBG have similar performance, incurring a performance degradation with respect to ideal channel estimation, which increases with the SNR since the slope of the curves is different. In other words, moving from RB/RBG to ideal channel estimation clearly provides a diversity gain to the system. Moreover, different precoders (cases (a) and (b)) have indistinguishable performance.

In Fig. 4, the BER is shown, as a function of the SNR, for the second simulation scenario in Table II, considering RI precoder, MMSE equalizer, and the presented channel estimation algorithms. In this case, the considered suboptimal algorithms incur a non-negligible SNR loss with respect to the ideal channel estimation. For instance, at $\mathrm{BER} = 10^{-3}$, the RB estimation algorithm incurs an energy loss of approximately 2.5 dB, whereas the RBG algorithm leads to an extra energy loss of approximately 0.5 dB. However, this comes with a significant gain in terms of amount of feedback information for channel estimation. In fact, in the ideal case $n_{\mathrm{f,ideal}} = 2400$ symbols, whereas RB and RBG need, respectively, $n_{\mathrm{f,RB}} = 200$ symbols and $n_{\mathrm{f,RBG}} = 72$ symbols, with a final saving between the ideal case and that with RBG estimation of approximately 97% of symbols. Therefore, RBG may actually represent a good tradeoff between channel estimation accuracy and

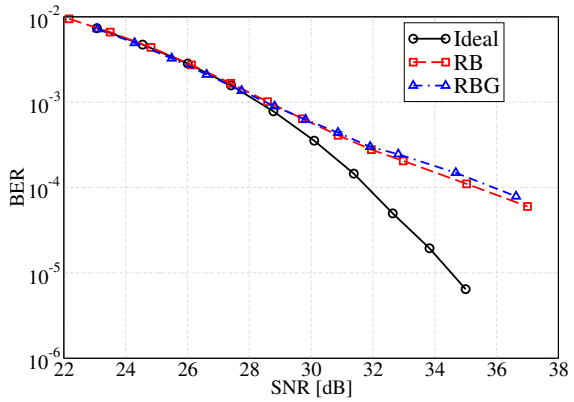

(a)

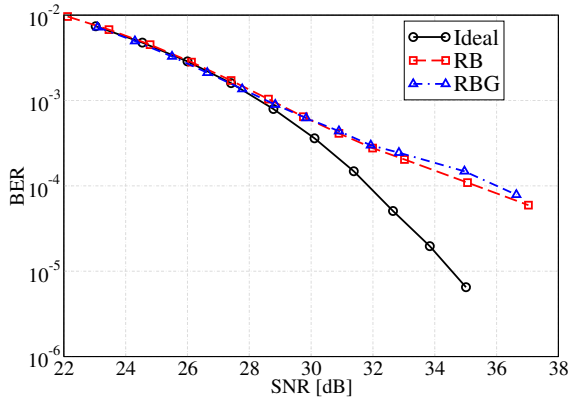

(b)

Fig. 3. BER, as a function of the SNR, for the first simulation scenario in Table II. The presented channel estimation algorithms are considered with MMSE equalizer and different precoders: (a) ZF and (b) RI.

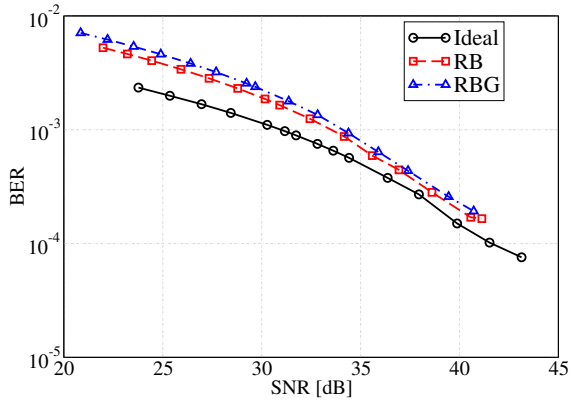

Fig. 4. BER, as a function of the SNR, for the second simulation scenario in Table II, considering RI precoder, MMSE equalizer, and the presented channel estimation algorithms.

amount of feedback information, especially if the MS can rely on advanced forward error correction schemes which could reduce the aforementioned SNR loss.

V. Concluding Remarks

In this paper, we analyzed the performance of two suboptimal channel estimation algorithms, denoted as RB and RBG, to be employed in a downlink MU-MIMO communication between a BS and multiple MSs. Communications are compliant with the LTE standard in FDD mode and are based on OFDM modulation. Since the LTE standard defines a fundamental block, denoted as PRB, consisting of a given number of 12 consecutive subcarriers in a time slot, the key idea is to approximate the channel as constant over multiples of this unit. This leads to a significant saving in terms of size of the feedback to be transmitted to the BS for precoding purposes, with minimal (often negligible) BER performance loss in all the considered scenarios.

References

[1] Cisco Systems, "Cisco visual networking index: Global mobile data traffic forecast update, 2016-2021," Tech. Rep., Feb. 2017, available at http://www.cisco.com/c/en/us/solutions/collateral/service-provider/ visual-networking-index-vni/mobile-white-paper-c11-520862.html.

[2] M. Agiwal, A. Roy, and N. Saxena, "Next generation 5G wireless networks: A comprehensive survey," *IEEE Commun. Surveys and Tutorials*, vol. 18, no. 3, pp. 1617–1655, third quarter 2016.

[3] A. Nordrum, "5G researchers set new world record for spectrum efficiency," *IEEE Spectrum*, May 2016, available at http://spectrum.ieee.org/techtalk/telecom/wireless/5gresearchers-achieve-new-spectrum-efficiency-record.

[4] "The LTE standard," Signals Research Group, Qualcomm, Tech. Rep., April 2014, Available at https://www.qualcomm.com/media/documents/files/the-lte-standard.pdf.

[5] L. Lu, G. Y. Li, A. L. Swindlehurst, A. Ashikhmin, and R. Zhang, "An overview of massive MIMO: Benefits and challenges," *IEEE J. Selected Topics Signal Proc.*, vol. 8, no. 5, pp. 742–758, Oct. 2014.

[6] J. Dai, A. Liu, and V. K. N. Lau, "FDD massive MIMO channel estimation with arbitrary 2D-array geometry," 2018, to appear in *IEEE Trans. Signal Processing*. Preprint available at http://ieeexplore.ieee.org/document/8298537.

[7] Z. Gao, L. Dai, W. Dai, B. Shim, and Z. Wang, "Structured compressive sensing-based spatio-temporal joint channel estimation for FDD massive MIMO," *IEEE Trans. Commun.*, vol. 64, no. 2, pp. 601–617, Feb. 2016.

[8] ETSI, "Technical Specification Group Radio Access Network-Evolved Universal Terrestrial Radio Access (E-UTRA)-Physical layer procedures," Tech. Rep., Oct. 2009, V8.8.0.

[9] N. Bhushan, T. Ji, O. Koymen, J. Smee, J. Soriaga, S. Subramanian, and Y. Wei, "Industry perspective: 5G air interface system design principles," *IEEE Wireless Commun.*, vol. 24, no. 5, pp. 6–8, Oct. 2017.

[10] J. Zyren, "Overview of the 3GPP long term evolution physical layer," NXP Semiconductors, Tech. Rep., Jul. 2007, available at https://www.nxp.com/docs/en/white-paper/3GPPEVOLUTIONWP.pdf.

[11] N. Fatema, G. Hua, Y. Xiang, D. Peng, and I. Natgunanathan, "Massive MIMO linear precoding: A survey," 2018, to appear in *IEEE Systems J.*. Preprint available at http://ieeexplore.ieee.org/document/8169014.

[12] A. Van Zelst and T. C. W. Schenk, "Implementation of a MIMO OFDM-based wireless LAN system," *IEEE Trans. Signal Processing*, vol. 52, no. 2, pp. 483–494, Feb. 2004.

[13] R. D. Gitlin, J. F. Hayes, and S. B. Weinstein, *Data Communications Principles*. New York, NY, USA: Springer-Verlag, 1992.

[14] ETSI, "Technical Specification Group Radio Access Network-Evolved Universal Terrestrial Radio Access (E-UTRA)-Base Station (BS) radio transmission and reception," Tech. Rep., Jul. 2010, V9.4.0.

[15] "ITU-R Recommendations, P.1238-7: Propagation data and prediction models for the planning of indoor radiocommunication systems and radio local area network in the frequency range 900 MHz to 100 GHz," 1997.